

Synthesis, Structure, and Photochemistry of 5,14-Diketopentacene

Tatsuya Aotake,^[a] Shinya Ikeda,^[b] Daiki Kuzuhara,^[b] Shigeki Mori,^[c] Tetsuo Okujima,^[a] Hidemitsu Uno,^[a] and Hiroko Yamada^{[b,d]*}**Keywords:** Pentacene / Photochemistry / Soluble precursor / Diketone / CT absorption

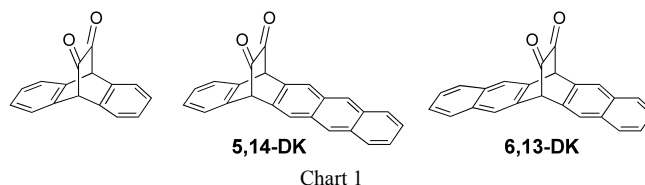
5,14- α -Diketopentacene, a structural isomer of 6,13- α -diketopentacene, was prepared from pentacene by three steps. Besides the typical $n-\pi^*$ absorption of C=O moiety around 468 nm and anthracene-like absorption at 333, 349, and 367 nm, a broad absorption was observed around 386 nm, which can be assigned to an intramolecular CT absorption from anthracene to C=O moiety. 5,14- α -Diketopentacene could be converted to pentacene quantitatively by photoirradiation at 405 nm and 468 nm in toluene with a quantum yield of 2.3 and 2.4%, respectively, and these

values are higher than 1.4% of 6,13- α -diketopentacene irradiated at 468 nm. The quantum yields in acetonitrile were lowered to 0.28 and 0.33% with irradiation at 468 and 405 nm. The crystal structure of 5,14- α -diketopentacene showed CH- π interaction and $\pi-\pi$ stacking between neighboring anthracene moieties and benzene moieties. The lower solubility of 5,14- α -diketopentacene compared to the 6,13-isomer could be explained by this crystal structure.

Introduction

The acenes, polycyclic aromatic hydrocarbons composed of linearly combined benzene units, have fascinated organic chemists for more than a century.^[1] Especially, pentacene (**PEN**) is a current choice in organic electronics such as organic thin-film transistors (OTFT)^[2-6] and organic thin-film photovoltaic cells.^[7-10] For the manufacture of the low-cost, easy-handling and printable devices, solution processing of the semiconducting materials is necessary. However, **PEN** is extremely insoluble in common organic solvents. Thus, soluble precursors with thermally or photochemically removable leaving groups have merited increasing attention.^[11-13] In this context, photochemical conversion of α -diketone precursor to anthracene leaving two CO molecules has been known for long time (Chart 1).^[14] By irradiation of diketone compounds at $n-\pi^*$ absorption, two molecules of CO are released and the corresponding acenes can be prepared quantitatively in solutions or in films. This reaction has recently been applied to the photochemical synthesis of **PEN** and larger acenes.^[15,16] Such a photochemical method has enabled us to prepare a thin film by a solution process using 6,13- α -diketone precursor of **PEN** (**6,13-DK**), followed by a simultaneous treatment with visible light and

mild heating. The thin film thus obtained exhibited top-contact OTFT with a mobility of $0.34 \text{ cm}^2 \text{ V}^{-1} \text{ s}^{-1}$ and on/off ratio of 2.0×10^6 . These values were comparable with those of devices prepared from thermally convertible precursors.^[17] In 2011, we reported the α -diketone precursor of monoanthraporphyrins.^[18] The photoirradiation of Soret band of the porphyrin moiety induced the decarbonylation of the connected α -diketone moiety and monoanthraporphyrin was obtained. In order to use this mechanism in the **PEN** system, we have designed 5,14- α -diketone precursor of **PEN** (**5,14-DK**), where anthracene moiety has the moderate absorbance besides the $n-\pi^*$ absorption and therefore the valid wavelength for the photoconversion from the precursor to **PEN** will be spread. Here we report the synthesis, crystal structures and photoreactivity of **5,14-DK**.

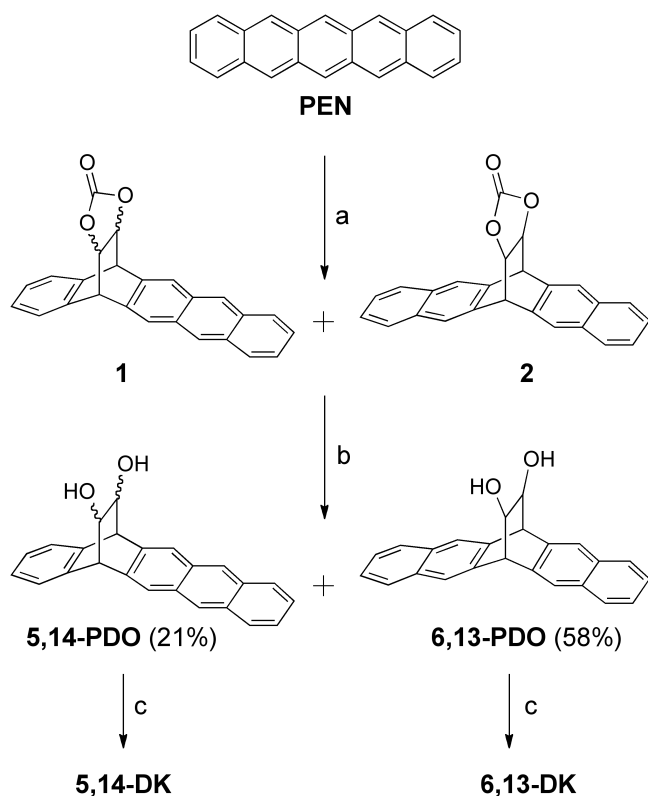


Results and Discussion

Synthesis The synthesis of **5,14-DK** is shown in Scheme 1. Diels-Alder reaction of vinylen carbonate with **PEN** gave a mixture of 5,14-adduct (**1**) and 6,13-adduct (**2**). After the deprotection of diol moieties, the mixture was separated by silica gel column chromatography to give 5,14-adduct (**5,14-PDO**) and 6,13-adduct (**6,13-PDO**) in 21% and 58%, respectively. Swern oxidation of **5,14-PDO** gave **5,14-DK** in 52% yield. The synthesis of **6,13-DK** has already been reported.^[15a,b]

- [a] Department of Chemistry and Biology, Graduate School of Science and Engineering, Ehime University, Matsuyama, 790-8577, Japan
 [b] Graduate School of Materials Science, Nara Institute of Science and Technology, Ikoma, 630-0192, Japan; Fax: +81-743-72-6041; E-mail: hyamada@ms.naist.jp
 [c] Department of Molecular Science, Integrated Center for Sciences, Ehime University, Matsuyama 790-8577, Japan
 [d] CREST, JST, Chiyoda-ku, 102-0075, Japan

Supporting information for this article is available on the WWW under <http://www.eurjoc.org/> or from the author.



Scheme 1. Reagents and conditions; i) vinylene carbonate, xylene, autoclave, 180 °C, 3 d.; ii) NaOH *aq.*, dioxane, reflux, 2 h, 21% for **5,14-PDO** and 58% for **6,13-PDO** for 2 steps.; iii) trifluoroacetic anhydride, *N,N*-diisopropylethylamine, *dry*-DMSO, *dry*-CH₂Cl₂, -60 °C, 1.5 h, 52% for **5,14-DK** and 43% for **6,13-DK**.

Crystal Structure X-ray-crystallographic measurement was performed on **5,14-DK** at 25 °C (Figures 1a).^[19] The angles made by C(9)–C(10)–C(11) and C(16)–C(17)–C(18) were 107.6(2)° and 106.7(1)° at 25 °C. The stacking pattern of the neighbouring molecules along the *c*-axis in the crystal was examined (Figure 1b). There was π - π overlap between two molecules. The distance of anthracene surfaces was 3.524 Å, which were shorter than the naphthalene-naphthalene surface distance of **6,13-DK** (3.596 Å).^[20] In general, anthracene has a stronger interaction between molecules than naphthalene. In **5,14-DK**, a similar interaction was observed between two molecules. The interaction was not only observed between the anthracene but also between the facing benzene rings. The surface distance of two benzene was 3.849 Å. In addition, there was CH- π interaction among hydrogen atoms and the neighbouring anthracene moiety. The shortest contact of hydrogen atoms and the anthracene surface is 2.767 Å. These interactions made the packing structure of **5,14-DK** rigid and lowered the solubility in common organic solvents. The solubility of **5,14-DK** in toluene was only 0.44 mg/mL at rt, although 2.3 mg/mL for **6,13-DK**.

Absorption Spectra UV-vis absorption spectra of **5,14-DK** and **6,13-DK** with the reference compounds **5,14-PDO**, **6,13-PDO** and **PEN** in toluene are shown in Figure 2a. The absorption spectra of **6,13-DK** shows n - π^* absorption of diketone moiety at 466 nm ($\epsilon = 1.22 \times 10^3 \text{ M}^{-1} \text{ cm}^{-1}$) and π - π^* absorption at 329 (4.23×10^3) and 315 (4.05×10^3) nm. The π - π^* absorption peaks of **6,13-PDO** are 321 (1.41×10^3) and 306 (1.22×10^3) nm. The π - π^* absorption peaks of **6,13-DK** are broader and red-shifted by 8 nm compared to those of **6,13-PDO**. For **5,14-DK**, a broad n - π^* absorption of

diketone moiety was observed at 464 nm (1.58×10^3) and π - π^* absorption of anthracene moiety observed at 333 (5.49×10^3), 349

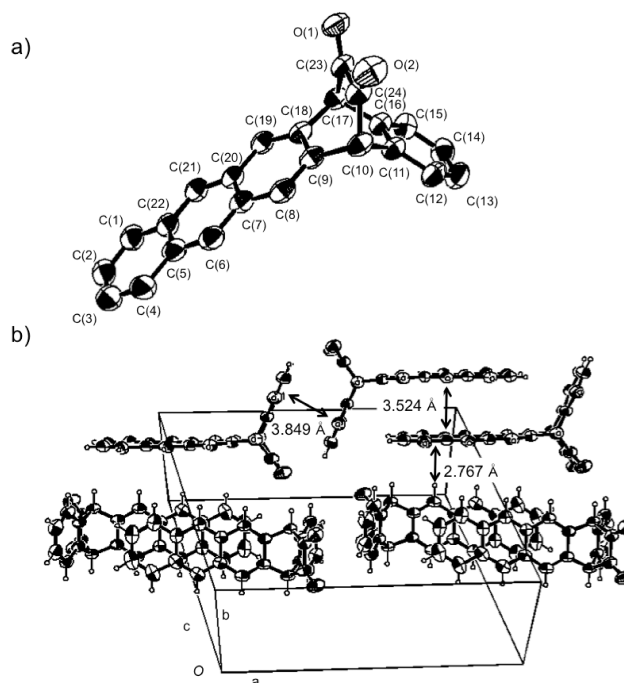


Figure 1. (a) ORTEP drawing of the X-ray structure of **5,14-DK** at 25 °C. Hydrogen atoms are omitted for clarity. Showing 30 % probability displacement ellipsoids. (b) Stacking pattern of neighbouring molecules.

(5.40×10^3), and 367 (4.20×10^3) nm. Furthermore a broad absorption at 386 nm (2.98×10^3) was observed, although the similar peak is not observed for **6,13-DK**. The edge or the broad band reached the n - π^* absorption, therefore the molar extinction coefficient of n - π^* absorption of **5,14-DK** is larger than that of **6,13-DK**. Compared to the absorption of **5,14-PDO**, the π - π^* absorption of anthracene moiety of **5,14-DK** is broadened and red-shifted by 7-8 nm, which means anthracene moiety of **5,14-DK** strongly interacts with carbonyl moieties.

The absorption at 386 nm was indigenous to **5,14-DK** and was not observed for **5,14-PDO**. The absorption spectra of **5,14-DK** were measured from 1.79×10^{-1} mM to 7.39×10^{-3} mM in toluene, but the concentration dependency was not observed. These phenomena suggested the absorption at 386 nm as an intramolecular charge-transfer (ICT) absorption from anthracene moiety to diketone moiety. To confirm it, the absorption spectra of **5,14-DK** were measured in toluene, dichloromethane, acetonitrile, and *N,N*-dimethylformamide (DMF) (Figure 2b). Additional to the π - π^* absorption at 333, 349, and 367 nm, the vibrational peak at 375 nm was observed with shoulders at 400 nm in DMF. In acetonitrile and DMF, the similar peaks were observed at 370 nm and 372 nm, respectively. The broad peak at 386 nm in toluene showed a clearer vibration structure compared with the other solvents; 382 nm (1.58×10^3) in dichloromethane, 382 (2.55×10^3) in DMF, and 379 nm (2.75×10^3) in acetonitrile with shoulders around 400 nm. The n - π^* absorption and π - π^* absorption at 333, 349, and 367 nm showed a slight solvent dependency. The molecular extinction efficiency of the peaks at 333, 349, and 367 nm were smaller than those in toluene, but the peaks were observed almost at the same wavelength. With an increase in polarity of the solvents, the peaks showed blue-shift. Therefore these peaks are assigned not as π - π^* absorption but as the ICT absorption.

Such an intramolecular interaction was not observed for **6,13-DK**, probably due to the difference in HOMO-level of anthracene and

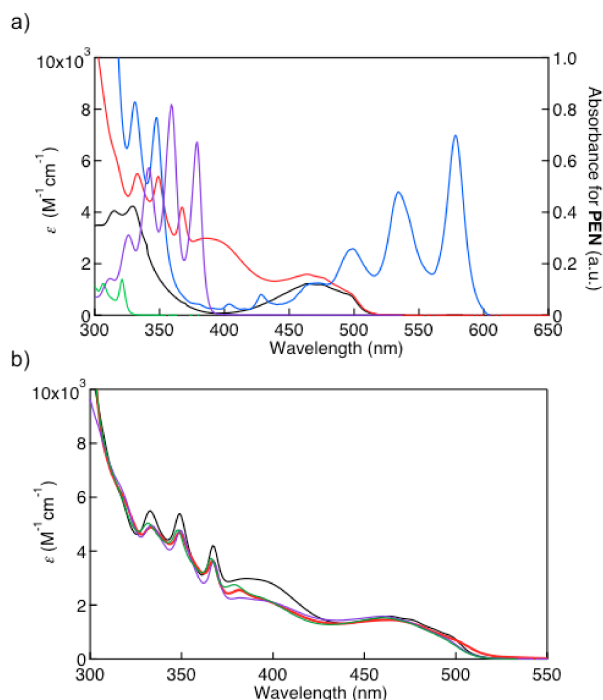


Figure 2. (a) UV/Vis absorption spectra of **5,14-DK** (red line), **6,13-DK** (black), **PEN** (blue), **5,14-PDO** (purple), **6,13-PDO** (green) in toluene. (b) Solvent effect of **5,14-DK**. In toluene (black), in dichloromethane (red), in acetonitrile (purple), in DMF (green).

naphthalene. The energy gap between HOMO level of naphthalene and LUMO level of diketone moiety is larger than that between HOMO level of anthracene and LUMO level of diketone moiety. Chow et. al. have reported the 6,13 and 5,14-monocarbonyl pentacene.^[13] In their system, CT-like absorption was not observed, since $n-\pi^*$ transition in the molecule is forbidden and the molar extinction coefficient was very small. For **5,14-DK** and **6,13-DK**, the molar extinction coefficients of $n-\pi^*$ absorption were over 1000 and the $n-\pi^*$ transition became possible to some extent.

MO and TD-DFT calculations were performed for **5,14-DK** using the Gaussian09 program package at the B3LYP/6-31G (d)//CAM-B3LYP/6-31G (d) level of theory (Figure 3). HOMO was localized to anthracene moiety, LUMO to carbonyl π^* orbital and HOMO-1 to the n orbital. TD-DFT calculations showed the absorption at 456 nm corresponded to $n-\pi^*$ transition that was mainly composed of the transition from HOMO-1 to LUMO (Figure S1). Also, the absorption at 358 nm was calculated as the transitions from HOMO to LUMO or LUMO+1, which corresponded to ICT from anthracene moiety to diketone moiety.

Photoreaction The photolysis reactions of α -diketone **5,14-DK** to pentacene in argon atmosphere are shown in Figure 4. **5,14-DK** was irradiated at $\lambda_{\text{ex}} = 405$ and 468 nm. To monitor the photoreaction process, the change in the UV/vis absorption spectra was measured every 30 s during photolysis. Firstly, the 1.1×10^{-1} mM toluene solution **5,14-DK** under an argon atmosphere was irradiated with light at 405 nm, as shown in Figure 4a. During irradiation, the peaks of 352–484 nm were decreased gradually, and new peaks at 495, 530, 578 nm were increased. After the absorption of **PEN** was increased for 25 min, a purple solid appeared in the solution. Judging from the observation of the isosbestic point at 352 and 484 nm, the photoreaction proceeded quantitatively.

Secondly, **5,14-DK** (1.3×10^{-1} mM) and **6,13-DK** (1.7×10^{-1} mM) in toluene under an argon atmosphere were irradiated with light at 468 nm, as shown in Figure 4b and S2. Similarly, the absorption

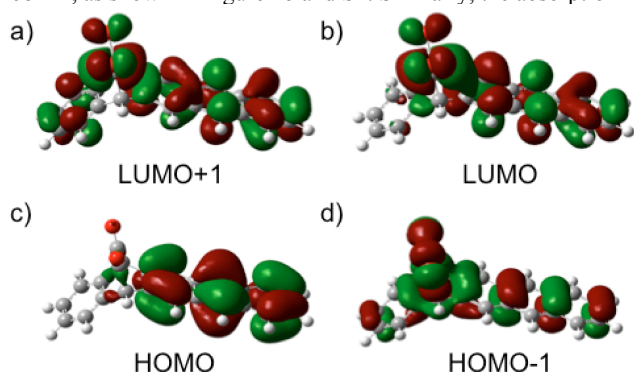
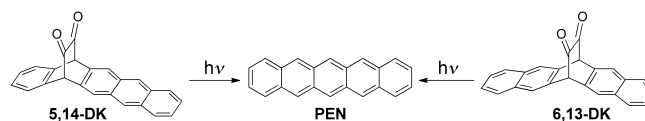


Figure 3. Molecular orbitals of (a) LUMO+1, (b) LUMO, (c) HOMO and (d) HOMO-1 of **5,14-DK** calculated at the B3LYP/6-31G(d) level.



Scheme 2. Photochemical conversion of α -diketone **5,14-DK** and **6,13-DK**.

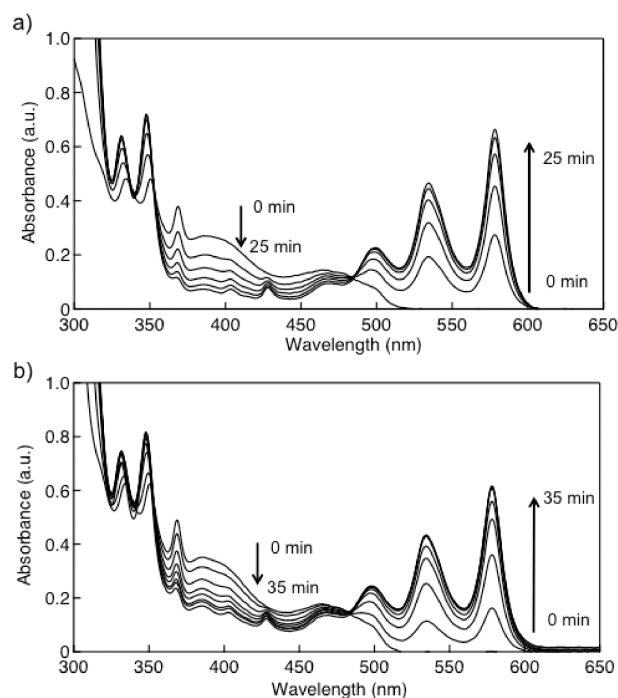


Figure 4. (a) The change in the absorption spectra during photolysis ($\lambda_{\text{ex}} = 405$ nm) of **5,14-DK** in toluene. (b) The change in the absorption spectra during photolysis ($\lambda_{\text{ex}} = 468$ nm) of **5,14-DK** in toluene.

spectra were changed from α -diketone to **PEN** with photoirradiation. The quantum yield of photoreaction (Φ_r) of **5,14-DK** was measured using potassium ferrioxalate actinometry (Table 1). The Φ_r of **5,14-DK** in toluene solution was determined to be 2.4% ($\lambda_{\text{ex}} = 405$ nm) and 2.3% (468 nm). The values were about two times that of **6,13-DK** (1.4%, 468 nm).

Next, the photolysis of **5,14-DK** and **6,13-DK** in acetonitrile were performed, as shown in Figure 5 and S3. In acetonitrile the photoreaction of **5,14-DK** was slower than that in toluene, and the Φ_r values were determined to be 0.28% for $\lambda_{\text{ex}} = 468$ nm and 0.33% for $\lambda_{\text{ex}} = 405$ nm, which were ten times lower than those in

toluene. The Φ_r value of **6,13-DK** irradiated at 468 nm in acetonitrile was 0.80%, lower than that of 1.4% in toluene. Similar behaviour of the solvent dependency of the reaction quantum yield was observed for the diketone precursor of monoanthraporphyrin.^[18] Compared with the photocleavage reaction in toluene, the occurrence of rapid photoinduced electron transfer from the singlet excited state porphyrin to the diketone moiety in benzonitrile resulted in a significant decrease in the singlet excited state lifetime, leading to prohibition of the photocleavage reaction.

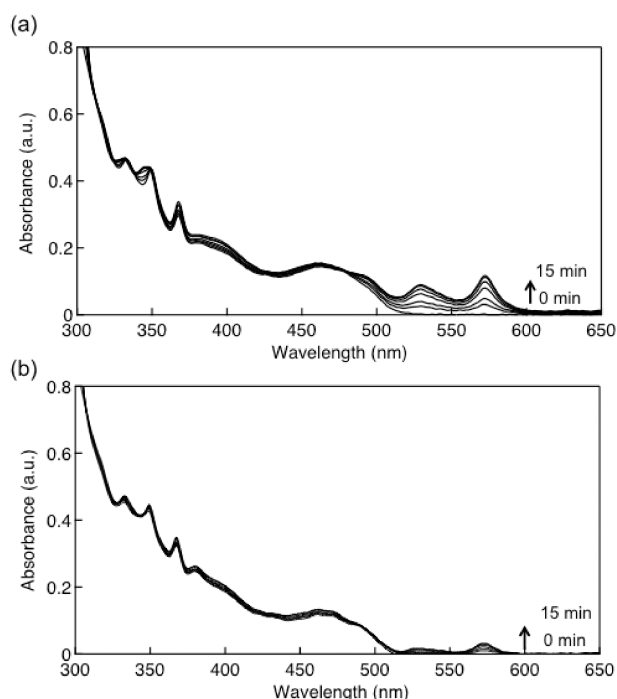


Figure 5. (a) The change in the absorption spectra during photolysis ($\lambda_{\text{ex}}=405$ nm) of **5,14-DK** in acetonitrile (b) The change in the absorption spectra during photolysis ($\lambda_{\text{ex}}=468$ nm) of **5,14-DK** in acetonitrile.

Table 1. Quantum yield of photoreactions of **5,14-DK** and **6,13-DK**

| | $\Phi_r\%$ | | | |
|----------------|------------|-----------|-----------------------|-----------------------|
| | toluene | | acetonitrile | |
| Excitation | 405 nm | 468 nm | 405 nm ^[a] | 468 nm ^[a] |
| 5,14-DK | 2.4 ± 1.0 | 2.3 ± 0.3 | 0.33 ± 0.13 | 0.28 ± 0.12 |
| 6,13-DK | – | 1.4 ± 0.3 | – | 0.80 ± 0.10 |

[a] The ϵ of **PEN** in acetonitrile was assumed same value in toluene.^[21]

The photoconversion was also performed in thin film. The UV spectra before and after the photoirradiation are shown in Figure S4 with the photos of the thin film. The yellow film was changed to purple by photoirradiation. However the spectrum of **5,14-DK** was broad and the band structures were not clear probably due to the π - π stacking of the compounds. The absorption spectrum of **PEN** was also broad, but the peaks typical for **PEN** were observed around 560 and 610 nm.^[15b]

Electrochemical Properties and Energy diagrams The electrochemical properties were measured in deaerated acetonitrile containing TBAPF₆, as shown in Figure S5 and S6. The one-electron reduction peak of **5,14-DK** was observed at -1.47 V (vs. Fc/Fc⁺) for the reduction of the diketone moiety. The oxidation peak was irreversible and the peak top was 0.94 V (vs. Fc/Fc⁺), which corresponded to the oxidation of the anthracene moiety. The energy level of the charge separated (CS) state (**Ant⁺-DK⁻**) was

determined from the redox potential. The driving forces ($-\Delta G_{\text{ET(CR)}}$) for the intramolecular charge-recombination processes from the anion radical of diketone moiety (**DK⁻**) to the cation radical of anthracene moiety (**Ant⁺**) were calculated by eqn (1),

$$-\Delta G_{\text{ET(CR)}} = e[E_{\text{ox}}(\text{Ant}^+/\text{Ant}) - E_{\text{red}}(\text{DK}/\text{DK}^-)] \quad (1)$$

where e stands for the elementary charge. On the other hand, the driving forces for the intramolecular charge-separation processes ($-\Delta G_{\text{ET(CS)}}$) from anthracene moiety (**Ant**) to the diketone singlet excited state (**¹DK***) was determined by eqn (2),

$$-\Delta G_{\text{ET(CS)}} = \Delta E_{0-0} + \Delta G_{\text{ET(CR)}} \quad (2)$$

where ΔE_{0-0} is the singlet excited state of diketone moiety (**¹DK***). The energy levels of **¹DK*** and **³DK*** were calculated from the anthracene diketone compounds already reported.^[22] The **¹DK*** and ICT (**(Ant-DK)***) levels were higher than the CS state level (-2.41 eV). Thus, electron transfer from **Ant** moiety to **DK** group may occur, affording the CS state, as shown in the α -diketone precursor of monoanthraporphyrins.^[18] The CS state decays mainly to the ground state by radiationless deactivation. However, the CS state in toluene may be higher in energy than in acetonitrile. Because of this, charge separation of **5,14-DK** is not favorable in toluene and the quantum yield of the photoreaction is higher than that in acetonitrile.

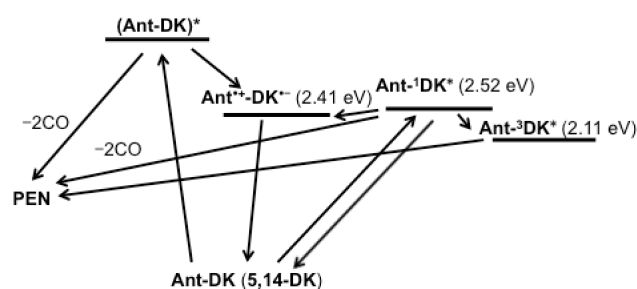


Figure 6. Energy diagram of **5,14-DK** in acetonitrile.

Conclusions

We successfully prepared a photo-convertible precursor of pentacene, **5,14-DK**, a structural isomer of **6,13-DK**. **5,14-DK** exhibited broad ICT absorption around 390 nm in addition to n - π^* absorption at 460 nm. The photochemical conversion to pentacene quantitatively proceeded by photoirradiation at ICT and n - π^* absorption in toluene, with a quantum yield of 2.4% and 2.3 %, respectively. However, the photoreaction in acetonitrile was slower with $\Phi_r = 0.33\%$ (405 nm) and 0.28% (468 nm), probably due to the occurrence of intramolecular charge transfer from **Ant** moiety to **DK** group. X-ray single crystal structure analysis of **5,14-DK** suggested that **5,14-DK** had strong π - π interaction with neighbouring molecules, which lowered the solubility of **5,14-DK** in common organic solvents.

Experimental Section

General Melting points were measured with a Yanaco M-500-D melting point apparatus and were not corrected. ¹H NMR and ¹³C NMR spectra were recorded on a JEOL JNM-AL 400 and AL 300 spectrometer at ambient temperature using tetramethylsilane as an internal standard. FAB mass spectra were measured on a JEOL JMS-MS700 spectrometer. UV-vis spectra were measured on a

JASCO UV/VIS/NIR Spectro-photometer V-570. Elemental analyses were performed on a Yanaco MT-5 elemental analyzer.

Materials Thin-layer chromatography (TLC) and gravity column chromatography were performed on Art. 5554 (Merck KGaA), and Silica Gel 60N (Kanto Chemical Co.), respectively. Acetonitrile was distilled from P₂O₅ *in vacuo*. All other solvents and chemicals were reagent grade quality, obtained commercially and used without further purification except as noted. For spectral measurements, spectral grade toluene, dichloromethane, acetonitrile and DMF were purchased from Nacalai tesque co.

Synthesis of 5,14-dihydro-15,16-dihydroxy-5,14-ethanopentacene (5,14-PDO) A solution of PEN (1.00 g, 3.60 mmol) and vinylene carbonate (0.310 g, 3.64 mmol) in xylene (68 ml) was mixed at 180 °C in an autoclave for 3 d. After removal of the solvent *in vacuo*, the residue was washed with EtOAc to give a mixture of carbonate compounds (1.29 g). The mixture of carbonate compounds (1.29 g, 3.55 mmol) was added to 4 M-NaOH *aq.* and 1,4-dioxane (40 ml). The resulting mixture was refluxed for 1 h. The reaction mixture was cooled, poured into water and then extracted with EtOAc. The combined organic layer was washed with water and dried over Na₂SO₄. After removal of the solvent *in vacuo*, the residue was purified by column chromatography on silica gel with EtOAc/CHCl₃ (1/4) to give **5,14-PDO** (0.260 g, 0.770 mmol, 21%) as white crystals, and 6,13-dihydro-15,16-dihydroxy-6,13-ethanopentacene **6,13-PDO** (0.710 g, 2.10 mmol, 58%). **5,14-PDO**; m.p. 275–277 °C. ¹H NMR (400 MHz, CDCl₃/TMS): δ = 2.18 (br, 2H, -OH), 4.23 (br, 2H), 4.56 (br, 2H), 7.25 (m, 2H), 7.44–7.72 (m, 2H), 7.89 (s, 2H), 7.97–7.95 (m, 2H), 8.33 (s, 2H) ppm. MS (FAB) *m/z*: 339 (M⁺+1); ¹³C NMR (100 MHz, CDCl₃/TMS) 51.26, 68.81, 122.79, 125.11, 125.70, 126.54, 127.00, 127.88, 136.80; Anal. Calcd for C₂₄H₁₈O₂: C, 85.18; H, 5.36. Found: C, 85.22; H, 5.30.

Synthesis of 5,14-dihydro-5,14-ethanopentacene-15,16-dione (5,14-DK) Trifluoroacetic anhydride (2.1 ml, 15.1 mmol) was added dropwise to a mixture of *dry*-DMSO (1.0 ml, 14.0 mmol) and *dry*-CH₂Cl₂ (10 ml) at –60 °C under an argon atmosphere. After stirring for 10 min, **5,14-PDO** (0.306 g, 0.905 mmol) dissolved in a mixture of *dry*-DMSO (10 ml) and *dry*-CH₂Cl₂ (7 ml) was added dropwise. After stirring for 90 min, *N,N*-diisopropylethylamine (4.50 ml, 25.8 mmol) was added dropwise to the reaction mixture. The solution was stirred for 60 min at –60°C, and warmed to rt. 3 M-HCl (50 ml) was added to the mixture. The mixture was extracted with CH₂Cl₂ and the organic layer was washed with water and brine, and dried over Na₂SO₄. After removal of the solvent *in vacuo*, the residue was purified by column chromatography on silica gel with CH₂Cl₂ and recrystallized from toluene to give **5,14-DK** as yellow crystals. (0.157 g, 0.469 mmol, 52%). m.p. > 300 °C. ¹H NMR (400 MHz, CDCl₃/TMS): δ = 5.19 (s, 2H), 7.39–7.41 (m, 2H), 7.48–7.52 (m, 4H), 7.99–8.01 (m, 2H), 8.07 (s, 2H), 8.42 (s, 2H) ppm. MS (FAB) *m/z*: 336 (M⁺+1); ¹³C NMR (75 MHz, CDCl₃/TMS) 60.46, 125.45, 126.03, 126.36, 126.50, 128.13, 129.60, 130.95, 131.21, 132.16, 134.90, 184.84; Anal. Calcd for C₂₄H₁₄O₂: C, 86.21; H, 4.22. Found: C, 86.50; H, 4.59.

Theoretical calculations All density functional theory calculations were achieved with the Gaussian09^[23] program package. The geometry was fully optimized at the Becke's three-parameter hybrid functional combined with the Lee-Yang-Parr correlation functional abbreviated as the B3LYP level of density functional theory with 6-31G(d) basis set. Equilibrium geometries were verified by the frequency calculations, where no imaginary frequency was found. Based on the B3LYP/6-31G(d) optimized

geometry, time dependent density functional theory (TDDFT) was conducted at the CAM-B3LYP/6-31G(d) level of theory.^[24]

Electrochemical measurements The cyclic voltammetry measurements of investigated compounds were performed on a BAS electrochemical analyser in deaerated acetonitrile containing *n*-Bu₄NPF₆ as a supporting electrolyte at 298 K (100 mV s⁻¹). The glassy carbon working electrode was polished with BAS polishing alumina suspension and rinsed with acetone before use. The counter electrode was a platinum wire. The measured potentials were recorded with respect to Ag/AgNO₃ and normalized to Fc/Fc⁺. **Photochemical reactions** The photocleavage reactions were carried out in a quartz UV cell which was irradiated by monochromatic excitation light through a monochromator (Ritsu MC-10N) by a 500 W xenon lamp (Ushio XB-50102AA-A) and monitored by OCEAN OPTICS high resolution spectrometer system HR-4000 with light source DH-2000-BAL. A standard actinometer (potassium ferrioxalate: K₃[Fe(C₂O₄)₃])^[25] was used for the quantum yield determination of the photochemical reactions of **5,14-DK** and **6,13-DK** in acetonitrile and toluene. A square quartz cuvette (10 mm i.d.) which contained a deaerated solution (3.0 cm³) of **5,14-DK** and **6,13-DK** was irradiated with monochromatized light of λ = 405 or 468 nm by a light through a monochromator (Ritsu MC-10N) using a 500W Xenon lamp (Ushio XB-50102AA-A). Under the conditions of actinometry experiments, the actinometer, both the **5,14-DK** or **6,13-DK** absorbed essentially all incident light. The photochemical reaction was monitored using a JASCO UV/VIS/NIR Spectrophotometer V-570. The quantum yields were determined from the increase in absorbance due to the PEN (578 nm) at the beginning of the reaction.

Photochemical reactions in film In 1ml of hot CHCl₃, 10mg of **5,14-DK** was dissolved. A 100 μl of the solution was spin coated on glass at 1000 rpm for 20 s. The absorption spectrum of the **5,14-DK** in film was measured. Then the film was irradiated with 460 W metalhalide lamp through blue filter in grove box for 90 min. Then the absorption spectrum of pentacene was measured.

X-ray analysis Single crystals of **5,14-DK** suitable for X-ray diffraction analysis were obtained by slow diffusion of heptane into a solution of **5,14-DK** in CH₂Cl₂. The crystals were mounted in Litho Loops (purchased from Protein Wave). The diffraction data was collected at 25 °C on a Rigaku VariMaxRAPID/a imaging plate diffractometer equipped graphite-monochromated CuKα radiation or on a Rigaku Mercury-8 diffractometer equipped graphite-monochromated MoKα radiation with a CCD detector. The diffraction data were processed with CrystalStructure on a Rigaku program, solved with the SIR-97 program,^[26] and refined with the SHELX-97 program.^[27]

Acknowledgments

The authors give thanks to Prof. Atsushi Wakamiya, Institute of Chemical Research, Kyoto University for his valuable discussion about TD-DFT calculation. This work was partially supported by Grants-in-Aid (No. 22350083 to H. Y.) and the Green Photonics Project in NAIST sponsored by the Ministry of Education, Culture, Sports, Science and Technology, MEXT, Japan. Leigh McDowel is highly acknowledged for English proof.

Supporting Information (see footnote on the first page of this article): . . .

- [1] a) M. Bendikov, F. Wudl, D. F. Perepichka *Chem. Rev.* **2004**, *104*, 4891-4946; b) J. E. Anthony *Chem. Rev.* **2006**, *106*, 5028-5048.
- [2] D. Knipp, R. A. Street, B. Krusor, R. Apte, J. Ho, *J. Non-cryst. Solids*, **2002**, *299-302*, 1042-1046.

- [3] a) H. Klauk, M. Halik, U. Zschieschang, G. Schmid, W. Radlik, W. Weber, *J. Appl. Phys.* **2002**, *92*, 5259-5263; b) H. Klauk, M. Halik, U. Zschieschang, F. Eder, G. Schmid, C. Dehm, *Appl. Phys. Lett.* **2003**, *82*, 4175-4177.
- [4] J. A. Nichols, D. J. Gundlach, T. N. Jackson, *Appl. Phys. Lett.* **2003**, *83*, 2366-2368.
- [5] M. Kitamura, T. Imada, Y. Arakawa, *Appl. Phys. Lett.* **2003**, *83*, 3410-3412.
- [6] D. Kumaki, M. Yahiro, Y. Inoue, S. Tokito, *Appl. Phys. Lett.* **2007**, *90*, 133511-3.
- [7] S. Yoo, B. Domerq, B. Kippelen, *Appl. Phys. Lett.* **2004**, *85*, 5427-5429.
- [8] J. Yang, T.-Q. Nguyen, *Org. Electr.* **2007**, *8*, 566-574.
- [9] J. Sakai, T. Taima, T. Yamanari, Y. Yoshida, A. Fujii, M. Ozaki, *Jpn. J. Appl. Phys.* **2010**, *49*, 032301-7.
- [10] K. Nomura, T. Oku, A. Suzuki, K. Kikuchi, G. Kinoshita, *J. Phys. Chem. Solids* **2010**, *71*, 210-213.
- [11] a) A. R. Brown, A. Pomp, D. M. de Leeuw, D. B. M. Klaassen, E. E. Havinga, P. Herwig, K. Müllen, *J. Appl. Phys.* **1996**, *79*, 2136-2138; b) P. T. Herwig, K. Müllen, *Adv. Mater.* **1999**, *11*, 480-483.
- [12] a) A. Afzali, C. D. Dimitrakopoulos, T. L. Breen, *J. Am. Chem. Soc.* **2002**, *124*, 8812-8813; b) A. Afzali, C. D. Dimitrakopoulos, T. O. Graham, *Adv. Mater.* **2003**, *15*, 2066-2069; c) K. P. Weidkamp, A. Afzali, R. M. Tromp, R. J. Hamers, *J. Am. Chem. Soc.* **2004**, *126*, 12740-12741; d) A. Afzali, C. R. Kagan, G. P. Traub, *Synth. Met.* **2005**, *155*, 490-494; e) D. Zander, N. Hoffmann, K. Lmimouni, S. Lenfant, C. Petit, D. Vuillaume, *Microelectron. Eng.* **2005**, *80*, 394-397; f) T. Akinaga, S. Yasutake, S. Sasaki, O. Sakata, H. Otsuka, A. Takahara, *Chem. Lett.* **2006**, *35*, 1162-1163.
- [13] a) K.-Y. Chen, H.-H. Hsieh, C.-C. Wu, J.-J. Hwang, T. J. Chow, *Chem. Commun.* **2007**, *10*, 1065-1067; b) T.-H. Chuang, H.-H. Hsieh, C.-K. Chen, C.-C. Wu, C.-C. Lin, P.-T. Chou, T.-H. Chao, T. J. Chow, *Org. Lett.* **2008**, *10*, 2869-2872.
- [14] J. Strating, B. Zwanenburg, A. Wagenaar, A. C. Udding, *Tetrahedron Lett.*, **1969**, *10*, 125-128.
- [15] a) H. Uno, Y. Yamashita, M. Kikuchi, H. Watanabe, H. Yamada, T. Okujima, T. Ogawa, N. Ono, *Tetrahedron Lett.* **2005**, *46*, 1981-1983; b) H. Yamada, Y. Yamashita, M. Kikuchi, H. Watanabe, T. Okujima, H. Uno, T. Ogawa, K. Ohara, N. Ono, *Chem. -Eur. J.* **2005**, *11*, 6212-6220; c) Y. Zhao, R. Mondal, D. C. Neckers, *J. Org. Chem.* **2008**, *73*, 5506-5513; d) S. Katsuta, H. Yamada, T. Okujima, H. Uno, *Tetrahedron Lett.* **2010**, *51*, 1397-1400.
- [16] a) R. Mondal, B. K. Shah, D. C. Neckers, *J. Am. Chem. Soc.* **2006**, *128*, 9612-9613; b) R. Mondal, R. M. Adhikari, B. K. Shah, D. C. Neckers, *Org. Lett.* **2007**, *9*, 2505-2508; c) R. Mondal, C. Tönshoff, D. Khon, D. C. Neckers, H. F. Bettinger, *J. Am. Chem. Soc.* **2009**, *131*, 14281-14289. d) C. Tönshoff, H. F. Bettinger, *Angew. Chem. Int. Ed.* **2010**, *49*, 4125-4128.
- [17] A. Masumoto, Y. Yamashita, S. Go, T. Kikuchi, H. Yamada, T. Okujima, N. Ono, H. Uno, *Jpn. J. Appl. Phys.* **2009**, *48*, 051505-5.
- [18] H. Yamada, D. Kuzuhara, K. Ohkubo, T. Takahashi, T. Okujima, H. Uno, N. Ono, S. Fukuzumi, *J. Mater. Chem.* **2010**, *20*, 3011-3024.
- [19] CCDC 854777 (25 °C) contain the supplementary crystallographic data for this paper. These data can be obtained free of charge from The Cambridge Crystallographic Data Center via www.ccdc.cam.ac.uk/data_request/cif.
- [20] At 25 °C the distance was 3.524 Å (Figure S5), which was also shorter than 3.596 Å of **6,13-DK**.
- [21] H-H. Perkampus in *UV-Vis Atlas of Organic Compounds. 2nd Ed.*, Weinheim; New York: VCH, **1992**, 652.
- [22] R. Mondal, A. N. Okhrimenko, B. K. Shah and D. C. Neckers, *J. Phys. Chem. B* **2008**, *112*, 11-15.
- [23] M. J. Frisch, G. W. Trucks, H. S. B. Schlegel, G. E. Scuseria, M. A. Robb, J. R. Cheeseman, G. Scalmani, V. Barone, B. Mennucci, G. A. Petersson, H. Nakatsuji, M. Caricato, X. Li, H. P. Hratchian, A. F. Izmaylov, J. Bloino, G. Zheng, J. L. Sonnenberg, M. Hada, M. Ehara, K. Toyota, R. Fukuda, J. Hasegawa, M. Ishida, T. Nakajima, Y. Honda, O. Kitao, H. Nakai, T. Vreven, J. A. Montgomery Jr., J. E. Peralta, F. Ogliaro, M. Bearpark, J. J. Heyd, E. Brothers, K. N. Kudin, V. N. Staroverov, R. Kobayashi, J. Normand, K. Raghavachari, A. Rendell, J. C. Burant, S. S. Iyengar, J. Tomasi, M. Cossi, N. Cossi, N. J. Millam, M. Klene, J. E. Knox, J. B. Cross, V. Bakken, C. Adamo, J. Jaramillo, R. Gomperts, R. E. Stratmann, O. Yazyev, A. J. Austin, R. Cammi, C. Pomelli, J. W. Ochterski, R. L. Martin, K. Morokuma, V. G. Zakrzewski, G. A. Voth, P. Salvador, J. J. Dannenberg, S. Dapprich, A. D. Daniels, . Ö. Farkas, J. B. Foresman, J. V. Ortiz, J. Cioslowski, D. J. Fox, et al. Gaussian 09 revision A.2, Gaussian, Inc.: Wallingford, CT, 2009.
- [24] a) A. D. Becke, *Phys. Rev. A* **1988**, *38*, 3098-3100; b) A. D. Becke, *J. Chem. Phys.* **1993**, *98*, 5648-5652; c) C. Lee, W. Yang, R. G. Parr, *Phys. Rev. B* **1988**, *37*, 785-789.
- [25] C. G. Hatchard, C. A. Parker, *Proc. R. Soc. Lond. A* **1956**, *235*, 518-536.
- [26] A. Altomare, M. C. Burla, M. Camalli, G. Cascarano, C. Giacovazzo, A. Guagliardi, A. G. G. Moliterni, G. Polidori, R. Spagna, *J. Appl. Crystallogr.* **1999**, *32*, 115-118.
- [27] G. M. Sheldrick, *Acta Crystallogr. A*, **2008**, *64*, 112-122.

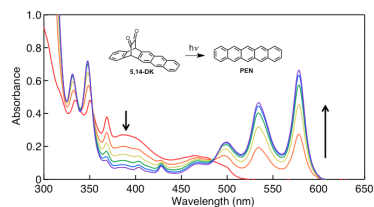
Received: ((will be filled in by the editorial staff))
Published online: ((will be filled in by the editorial staff))

Entry for the Table of Contents ((Please choose one layout.))

Layout 1:

((Key Topic))

5,14- α -Diketopentacene prepared from pentacene in three steps could be converted to pentacene by photoirradiation. The irradiation at n- π^* absorption and intramolecular charge transfer state gave pentacene at the quantum yields of 2.3 and 2.4%, respectively.



Tatsuya Aotake, Shinya Ikeda, Daiki Kuzuhara, Shigeki Mori, Tetsuo Okujima, Hidemitsu Uno and Hiroko Yamada Page No. – Page No.

Synthesis, Structure, and Photochemistry of 5,14-Diketopentacene

Keywords: ((Photochemistry / Soluble precursor / Diketone / Pentacene / Absorption))

Supporting Information

Synthesis, Structure, and Photochemistry of 5,14-Diketopentacene

**Tatsuya Aotake,^[a] Shinya Ikeda,^[b] Daiki Kuzuhara,^[b] Shigeki Mori,^[c] Tetsuo Okujima,^[a]
Hidemitsu Uno,^[a] and Hiroko Yamada^{[b,d]*}**

[a] Department of Chemistry and Biology, Graduate School of Science and Engineering, Ehime University, Matsuyama, 790-8577, Japan

[b] Graduate School of Materials Science, Nara Institute of Science and Technology, Ikoma, 630-0192, Japan; Fax: +81-743-72-6041; E-mail: hyamada@ms.naist.jp.

[c] Department of Molecular Science, Integrated Center for Sciences, Ehime University, Matsuyama 790-8577, Japan

[d] CREST, JST, Chiyoda-ku, 102-0075, Japan

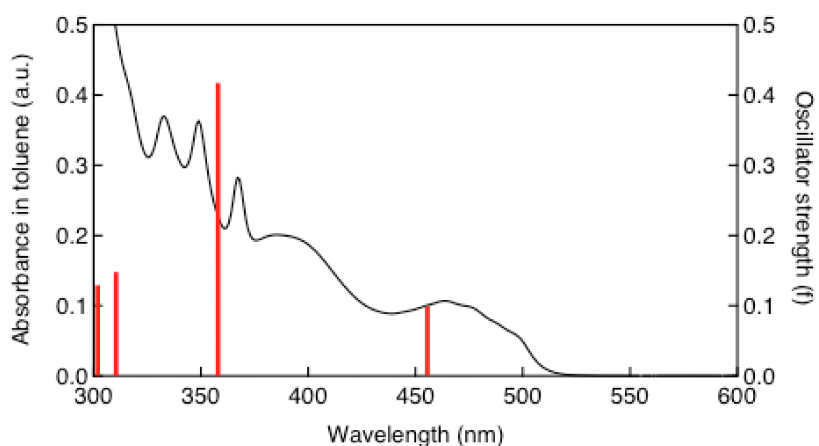


Figure S1. TD-DFT calculation at B3LYP/6-31G(d)//CAM- B3LYP/6-31G(d). In toluene (black), TD-DFT calculation (red bar).

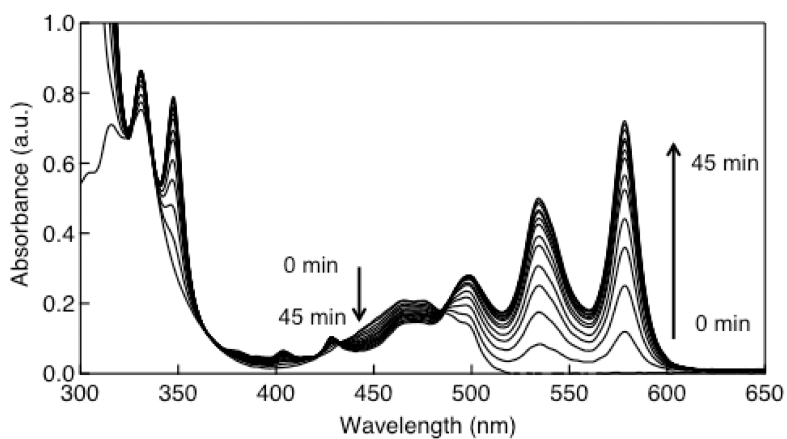


Figure S2. Change in absorption spectra during photolysis ($\lambda_{\text{ex}} = 468 \text{ nm}$) of **6,13-DK** in toluene.

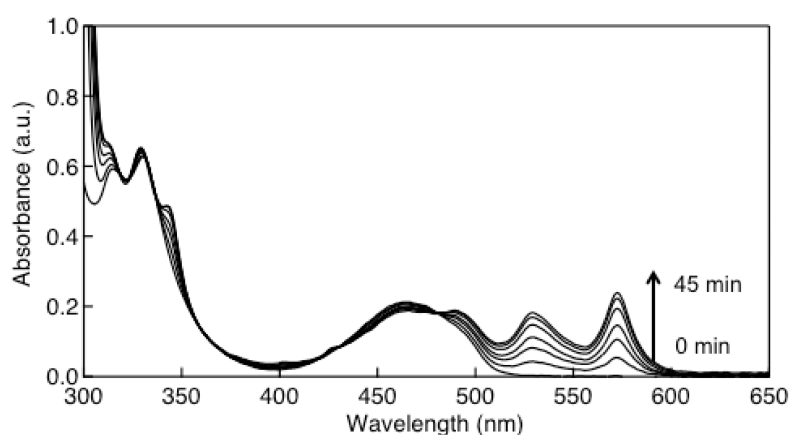


Figure S3. Change in absorption spectra during photolysis ($\lambda_{\text{ex}} = 468 \text{ nm}$) of **6,13-DK** in acetonitrile.

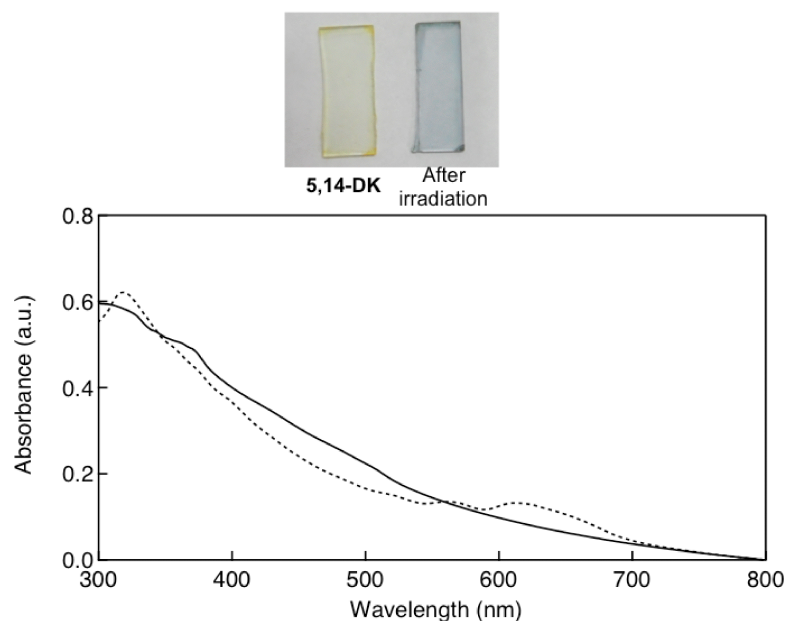


Figure S4. Change in absorption spectra in films. **5,14-DK** (solid) and after irradiation (dotted).

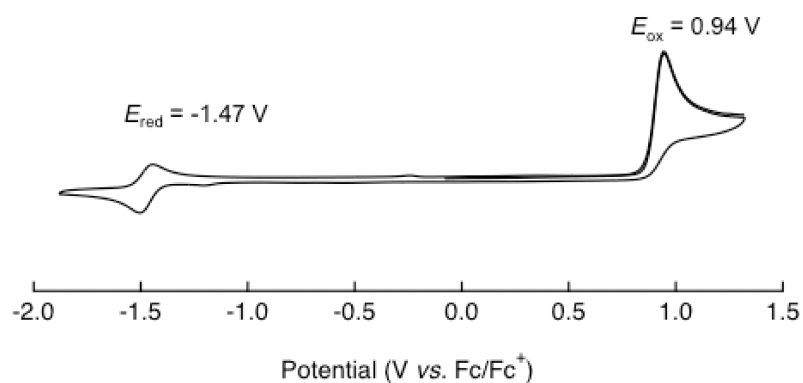


Figure S5. Cyclic voltammogram of **5,14-DK**. In 0.1 M TBAPF₆ in acetonitrile. Scan rate 0.1 V / s. [diketone] = 0.1 mM. WE: glassy carbon, CE: Pt, RE: Ag/AgNO₃. *Oxidation potential is peak top.

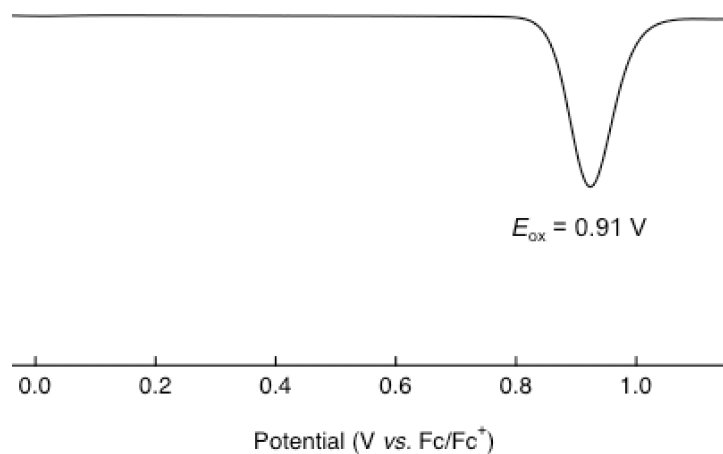


Figure S6. DPV of **5,14-DK**. In 0.1 M TBAPF₆ in acetonitrile. [diketone] = 0.1 mM. WE: glassy carbon, CE: Pt, RE: Ag/AgNO₃.

Cartesian coordinates and vibrational frequencies for the optimized structure of 5,14-DK

E(RB3LYP) = -1073.46409943 A.U.

Stoichiometry C₂₄H₁₄O₂

Framework group C1[X(C₂₄H₁₄O₂)]

Deg. of freedom 114

Full point group C1 NOp 1

Largest Abelian subgroup C1 NOp 1

Largest concise Abelian subgroup C1 NOp 1

Standard orientation:

| Center Number | Atomic Number | Atomic Type | Coordinates (Angstroms) | | |
|---------------|---------------|-------------|-------------------------|-----------|-----------|
| | | | X | Y | Z |
| 1 | 6 | 0 | 6.493245 | -0.397489 | 0.712762 |
| 2 | 6 | 0 | 6.493252 | -0.397385 | -0.712806 |
| 3 | 6 | 0 | 5.317269 | -0.291477 | -1.407322 |
| 4 | 6 | 0 | 4.067828 | -0.178743 | -0.722342 |
| 5 | 6 | 0 | 4.067821 | -0.178849 | 0.722316 |
| 6 | 6 | 0 | 5.317259 | -0.291686 | 1.407287 |
| 7 | 6 | 0 | 2.848694 | -0.067148 | -1.403773 |
| 8 | 6 | 0 | 1.631148 | 0.045286 | -0.723343 |
| 9 | 6 | 0 | 1.631144 | 0.045198 | 0.723340 |
| 10 | 6 | 0 | 2.848687 | -0.067337 | 1.403759 |
| 11 | 6 | 0 | 0.383612 | 0.165879 | -1.414854 |
| 12 | 6 | 0 | -0.788356 | 0.264645 | -0.718547 |
| 13 | 6 | 0 | -0.788355 | 0.264575 | 0.718579 |
| 14 | 6 | 0 | 0.383612 | 0.165732 | 1.414868 |
| 15 | 6 | 0 | -2.177183 | 0.422155 | -1.322295 |
| 16 | 6 | 0 | -3.097439 | -0.623219 | -0.703446 |
| 17 | 6 | 0 | -3.097428 | -0.623302 | 0.703394 |
| 18 | 6 | 0 | -2.177195 | 0.422013 | 1.322343 |
| 19 | 6 | 0 | -3.914228 | -1.507143 | -1.405005 |
| 20 | 6 | 0 | -4.724109 | -2.400366 | -0.698473 |
| 21 | 6 | 0 | -4.724101 | -2.400450 | 0.698217 |
| 22 | 6 | 0 | -3.914215 | -1.507313 | 1.404851 |
| 23 | 6 | 0 | -2.702413 | 1.765624 | 0.780918 |
| 24 | 6 | 0 | -2.702368 | 1.765724 | -0.780731 |
| 25 | 8 | 0 | -3.069165 | 2.706346 | 1.442091 |
| 26 | 8 | 0 | -3.069286 | 2.706453 | -1.441800 |
| 27 | 1 | 0 | 7.435580 | -0.482084 | 1.245883 |
| 28 | 1 | 0 | 7.435590 | -0.481909 | -1.245930 |
| 29 | 1 | 0 | 5.315040 | -0.290534 | -2.494164 |
| 30 | 1 | 0 | 5.315033 | -0.290900 | 2.494129 |
| 31 | 1 | 0 | 2.848939 | -0.065627 | -2.491360 |
| 32 | 1 | 0 | 2.848941 | -0.065957 | 2.491346 |
| 33 | 1 | 0 | 0.385362 | 0.177269 | -2.501913 |
| 34 | 1 | 0 | 0.385381 | 0.177016 | 2.501928 |
| 35 | 1 | 0 | -2.181942 | 0.422477 | -2.413251 |
| 36 | 1 | 0 | -2.181938 | 0.422237 | 2.413298 |
| 37 | 1 | 0 | -3.918964 | -1.501078 | -2.491370 |
| 38 | 1 | 0 | -5.358783 | -3.095660 | -1.239623 |
| 39 | 1 | 0 | -5.358774 | -3.095802 | 1.239294 |
| 40 | 1 | 0 | -3.918951 | -1.501373 | 2.491217 |

Harmonic frequencies (cm⁻¹), IR intensities (KM/Mole), Raman scattering activities (A⁴/AMU), depolarization ratios for plane and unpolarized incident light, reduced masses (AMU), force constants (mDyne/A), and normal coordinates:

| | 1 | 2 | 3 |
|----------------|---------|---------|---------|
| | A | A | A |
| Frequencies -- | 31.4415 | 60.6010 | 75.4920 |
| Red. masses -- | 6.5606 | 4.4522 | 6.7917 |
| Frc consts -- | 0.0038 | 0.0096 | 0.0228 |
| IR Inten -- | 0.5588 | 0.1785 | 0.1330 |